Self-Assembly of a Water-Soluble Pd_{16} Square Bicupola Architecture and Its Use in Aerobic Oxidation in Aqueous Medium

Pranay Kumar Maitra, Soumalya Bhattacharyya, Neal Hickey, and Partha Sarathi Mukherjee*

ABSTRACT: Designing supramolecular architectures with uncommon geometries has always been a key goal in the field of metal–ligand coordination-driven self-assembly. It acquires added significance if functional building units are employed in constructing such architectures for fruitful applications. In this report, we address both these aspects by developing a water-soluble $Pd_{16}L_8$ coordination cage **1** with an unusual square orthobicupola geometry, which was used for selective aerobic oxidation of aryl sulfides. Self-assembly of a benzothiadiazole-based tetra-pyridyl donor **L** with a ditopic *cis*-[(tmeda)Pd(NO_3)$_2$] acceptor [tmeda = *N*,*N*,*N*′,*N*′-tetramethylethane-1,2-diamine] produced **1**, and the geometry was determined by single-crystal X-ray diffraction study. Unlike the typically observed tri- or tetrafacial barrel, the present $Pd_{16}L_8$ coordination assembly features a distinctive structural topology and is a unique example of a water-soluble molecular architecture with a square orthobicupola geometry. Efficient and selective aerobic oxidation of sulfides to sulfoxides is an important challenge as conventional oxidation generally leads to the formation of sulfoxide along with toxic sulfone. Cage **1**, designed with a ligand containing a benzothiadiazole moiety, demonstrates an ability to photogenerate reactive oxygen species (ROS) in water, thus enabling it to serve as a potential photocatalyst. The cage showed excellent catalytic efficiency for highly selective conversion of alkyl and aryl sulfides to their corresponding sulfoxides, therefore without the formation of toxic sulfones and other byproducts, under visible light in aqueous medium.

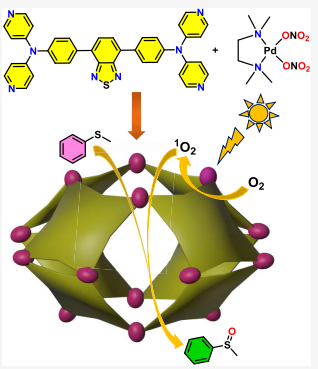

INTRODUCTION

Enzymes utilize weak noncovalent interactions, especially within substrate-binding pockets, to regulate complex biochemical processes.[1] This natural mechanism has inspired synthetic chemists to create supramolecular architectures of various shapes, sizes, and functionalities that mimic enzymatic functions.[2] Substrate encapsulation in such structures elevates the reaction rate by enhancing substrate concentration through proximity effects, reducing entropy, and meticulously preorganizing reactants. Numerous molecular containers featuring precisely defined cavities have already been reported in pursuit of this goal.[3] Metal–ligand coordination-driven self-assembly is a highly effective approach for synthesizing intricate supramolecular architectures. It also utilizes diverse precursors with different bite angles, making it a preferred choice among various noncovalent self-assembly processes. The resulting supramolecular architectures find applications in supramolecular catalysis,[4] drug delivery,[5] light harvesting,[6] and photoswitching.[7]

In the past two decades, there has been a significant advancement in the discovery of various architectures through this strategy of metal–ligand coordination-driven self-assembly.[8] Particularly, the synthesis of coordination cages has seen notable progress by strategically employing *cis*-blocked Pd(II) or Pt(II) complexes.[9] These complexes have a unique configuration with two available coordination sites at an angle of 90°. The interaction between these metal complexes and tetratopic rigid N-donor ligands has been extensively explored, establishing it as a well-researched and effective approach in synthetic chemistry.[10] Self-assembly of such tetratopic rigid donors (D) with *cis*-blocked Pd/Pt acceptors (M = Pd/Pt) has been found to yield mainly tetrafacial (M_8D_4) and trifacial (M_6D_3) barrels.[11] Notably, elongating the ligand length by modifying the spacer group in a supramolecular system has proven to be an effective method in creating more intricate structures.[12] These include larger supramolecular cages with spacious pockets suitable for guest encapsulation and catalysis.[13] Along with the attractive structural features, a significant amount of research has been dedicated to develop water-soluble, larger self-assembled coordination complexes for solving challenging problems in aqueous medium. One such challenging and important problem is the efficient, selective oxidation of sulfides to sulfoxides, therefore without producing toxic sulfones and other byproducts, under mild reaction conditions. This is of enormous significance as sulfoxides play a crucial role in

Scheme 1. Schematic Representation of the Synthesis of 1

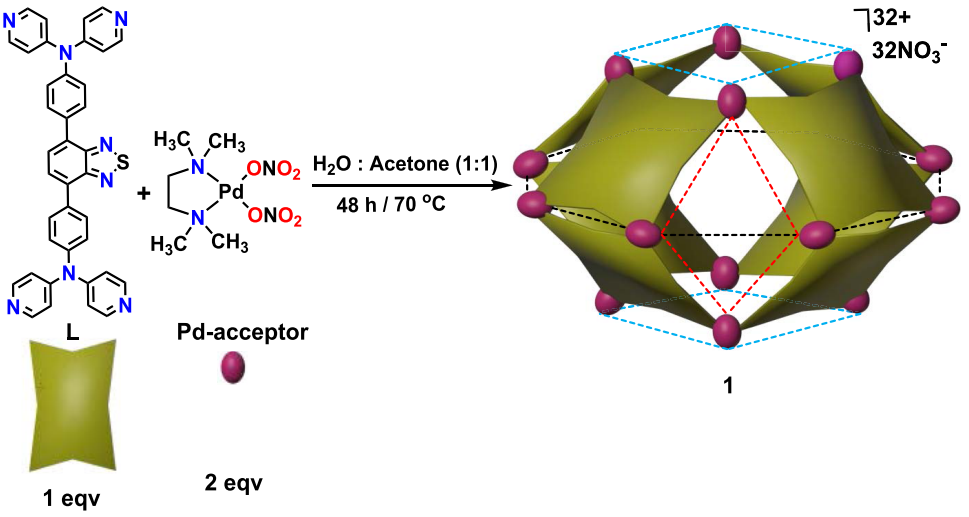

organic synthesis,[14] pharmaceuticals,[15] and polymers.[16] Some sulfoxides, such as those found in drugs such as omeprazole and sulindac, exhibit notable pharmacological properties. Current methods for sulfoxide synthesis often involve the use of multiple oxidants, leading to excessive waste, and pose challenges in terms of selectivity with the risk of forming undesired sulfones. Additionally, many existing protocols require high temperature.[17] In this regard, it is appealing to develop a self-assembled cage with a unique geometry, using a functional ligand motif, for selective photooxidation of sulfides to sulfoxides in high yields under aerobic and aqueous conditions.

Herein, we report the synthesis of a very large Pd_{16} architecture (**1**) by the self-assembly of a tetra-pyridyl donor (**L**) containing a benzothiadiazole core with a *cis*-Pd(II) acceptor (Scheme 1). The Pd_{16} cage (**1**) shows the distinctive structural topology of the Johnson solid J_{28}. This topology represents a square orthobicupola geometry, which is unusual, and to the best of our knowledge, cage **1** is the first example of a water-soluble Pd(II) molecular architecture with a square orthobicupola geometry. This cage **1** exhibits robust light absorption characteristics in the visible spectrum, and it contains the photosensitizing benzothiadiazole units in the backbone, thus enabling the cage to be fluorescent and active for reactive oxygen species (ROS) generation upon exposure to visible light in aqueous medium. **1** was found to be efficient for selective aerial oxidation of sulfides to their corresponding sulfoxides, with excellent catalytic activity under aqueous medium and without the formation toxic byproducts. Furthermore, the cage could be reused for multiple cycles without any significant loss of catalytic activity.

RESULTS AND DISCUSSION

A Suzuki coupling reaction was utilized to synthesize the new tetra-pyridyl ligand **L** involving the compounds 4,7-bis(4,4,5,5-tetramethyl-1,3,2-dioxaborolan-2-yl)benzo[*c*] [1,2,5]thiadiazol (a) and *N*-(4-iodophenyl)-*N*-(pyridin-4-yl)pyridin-4-amine (b) (Scheme 2). The final product (**L**) was isolated and characterized by multinuclear NMR (Figures S2−S4) and electrospray ionization mass spectrometry (ESI-MS) analyses (Figure S5).

The synthesis of nanocage **1** involved a combination of **L** and *cis*-[(tmeda)Pd(NO_3)$_2$] in 1:2 ratio in a water/acetone

Scheme 2. Schematic Presentation on the Synthesis of the Ligand L

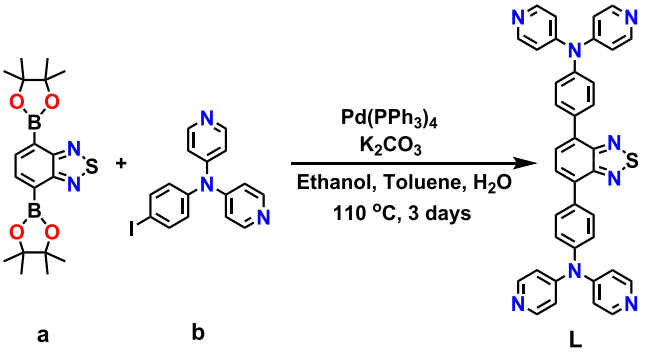

mixture (1:1) and reacting at 70 °C for 48 h. The outcome of this reaction was the formation of a distinct and clear orange solution (Scheme 1). The orange solution was evaporated to dryness and recrystallized by diffusing acetone into an aqueous solution of the product to give a yield of 85%. Notably, while the resulting self-assembled product (**1**) is soluble in water, its building block **L** is not. The ^{1}H NMR spectrum of **1** in D_2O displayed 12 distinct peaks in the aromatic region, spanning from 6.91 to 9.05 ppm. On the other hand, the building block **L** showed the expected five peaks in the aromatic region (Figure 1). Such splitting in the ^{1}H NMR of **1** compared to **L** suggests a complex structure resulting in different chemical environments of the protons of **1**. After a detailed examination of the spectrum, it became clear that there are three unique sets of α-pyridyl protons with 1:2:1 integration ratio and four distinct sets of β-pyridyl protons displaying 1:1:1:1 integration ratio. This division in signals indicates that each of the four protons in every pyridyl ring of the ligand encounters a unique chemical environment. This could be due to the presence of an unconventional structure. Appearance of a complex NMR spectrum eliminated the formation of the anticipated simple barrel structure with three or four faces, as barrels are expected to give a simple NMR spectrum. Identification of the peaks was facilitated with the help of ^{1}H−^{1}H COSY (Figure S7). The occurrence of multiple proton peak splittings in the ^{1}H NMR spectrum could be attributed to the presence of multiple assemblies. However, the single diffusion band with a log *D*

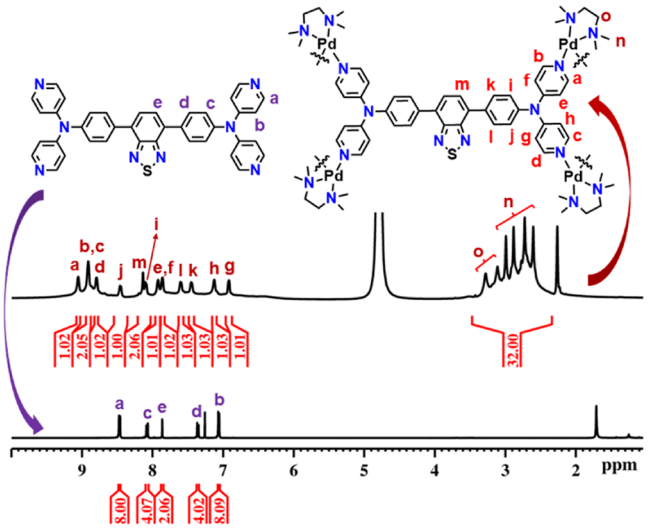

Figure 1. Stacked ^{1}H NMR spectra of ligand **L** (in $CDCl_3$, bottom) and cage **1** (in D_2O, top).

value of −10.08 observed in the ^{1}H-DOSY analysis confirmed the existence of a single molecular entity (Figure S8).

For better ionization under electrospray ionization (ESI), nitrate counteranions in **1** were exchanged with PF_6^- by treating **1** with excess KPF_6 in a 1:1 mixture of water and acetone. An ESI mass spectrometry (ESI-MS) investigation was performed on this PF_6^- analogue in acetonitrile. The results revealed several distinct peaks with notable abundances at m/z values of 1506.7876, 1323.256, 1176.4364, and 1056.3127 (Figure 2) with correct isotopic patterns corresponding to the charged fragments $[\mathbf{1}\text{-}8PF_6^-]^{8+}$, $[\mathbf{1}\text{-}9PF_6^-]^{9+}$, $[\mathbf{1}\text{-}10PF_6^-]^{10+}$, and $[\mathbf{1}\text{-}11PF_6^-]^{11+}$, respectively (Figure S9), which confirm the formation of an $M_{16}L_8$ assembly.

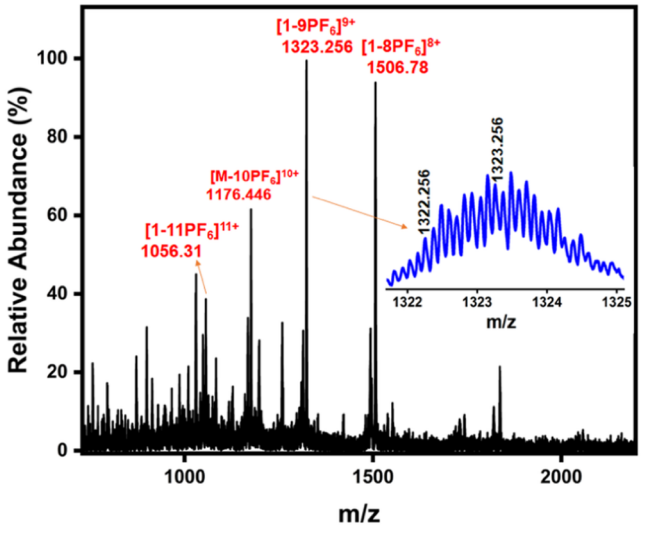

Figure 2. ESI-MS spectrum of the PF_6^-analogue of **1** in acetonitrile. (Inset) Isotopic distribution pattern of the $[\mathbf{1}\text{-}9PF_6^-]^{9+}$ fragment.

Although the NMR and mass spectrometric analyses confirmed the presence of a single $M_{16}L_8$ assembly, they failed to provide the exact arrangement of the ligands and the overall structure of the assembly. Diffraction-quality single crystals of **1** were obtained by the slow diffusion of acetone vapor into a concentrated aqueous solution of compound **1** (nitrate analogue). X-ray diffraction data were collected from an appropriate single crystal using synchrotron radiation. The analysis of the data unequivocally confirmed the existence of a distorted square orthobicupola geometry ($\mathbf{M_{16}L_8}$) (Figure 3).

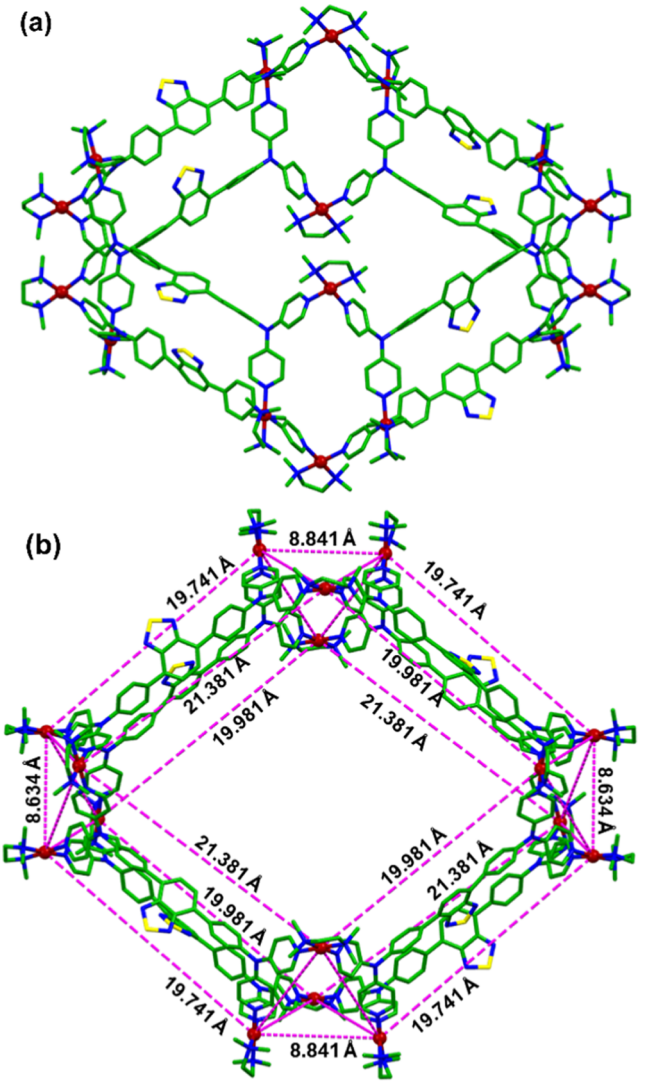

Figure 3. (a, b) Capped-stick representation of the X-ray crystal structure of cage **1** (side view) and top view of nanocage **1** (color codes: C = green, N = blue, Pd = red, and S = yellow).

The square orthobicupola geometry is classified as one of the Johnson polyhedral solids, specifically the J_{28} polyhedron, composed of 10 squares and 8 equilateral triangles. This is a unique example of a Pd(II) coordination architecture with such unusual structural topology, showing water solubility.

This distorted square orthobicupola (**1**) crystallized in the centrosymmetric monoclinic space group $C2/m$. Although the structure classifies as a square orthobicupola, none of the faces are in fact square and, therefore, the triangles are not equilateral. Further details of the geometry of the structure defined by the Pd(II) ions are outlined in the Supporting Information (Figure S1 and Table S2). For cage **1**, a tetratopic ligand **L** is paneled on 8 of the 10 quadrilateral faces. The remaining two faces are open and positioned opposite to each other, thus making it a structure with two large, identical open windows. The sides of the windows differ in length by about

0.14 nm and each of the windows has an opening greater than 3 nm, measured as the maximum diagonal Pd−Pd distance. Such a value is significantly larger than the diameter of the usual $M_{2n}L_n$ barrels.

The photophysical characteristics of cage **1** were investigated in deionized water. Cage **1** exhibited two absorption peaks at wavelengths of 339 and 400 nm, corresponding to $\pi-\pi^*$ and $n-\pi^*$ transitions, respectively. In an aqueous environment, **1** displayed fluorescence emission with a Stokes shift of 130 nm and an absolute quantum yield (QY) of 20.81% (Figure 4a,b).

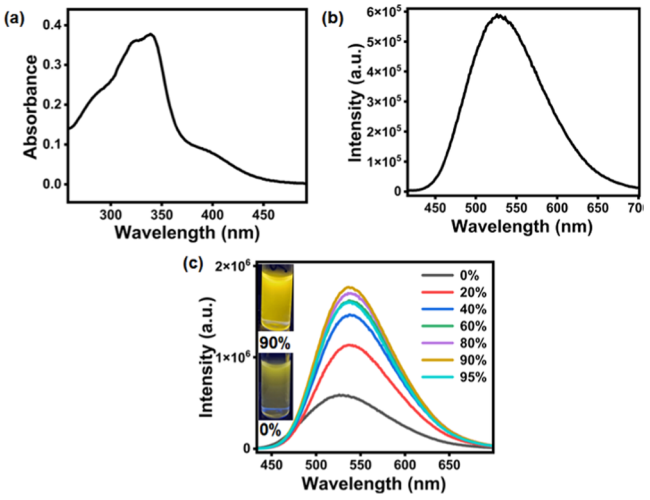

Figure 4. (a) Absorption spectrum of **1** in 10 μM aqueous solution. (b) Emission spectrum of **1** upon excitation at 400 nm. (c) Change in the fluorescence spectrum of **1** with increasing CH_3CN fraction in water solution (λ_{ex} = 400 nm).

This is a remarkable value for a dilute aqueous solution of Pd(II) complex. Although the emission is quite high for a Pd(II)-based complex, it is not comparable to highly emissive chromophores, primarily due to nonradiative decay. However, adding acetonitrile to an aqueous solution of nanocage **1** gives rise to aggregation-induced emission (AIE) (Figure 4c). This is attributed to the increased restriction of phenyl ring rotation in the aggregated state. Notably, in a 90% acetonitrile/water mixture, cage **1** demonstrates a significant enhancement in emission, reaching a threefold increase in intensity compared to the water-only solution, with a significantly high quantum yield of 70.39% (Figures S10−S11). The morphology of the supramolecular aggregate of **1** was investigated by using scanning electron microscopy (SEM), which revealed the formation of spherical nanoparticles (Figure S12). Such a highly luminescent self-assembled cage based on Pd(II) is a rare occurrence.

Benzothiadiazole-based fluorophores show significant promise as materials for generating reactive oxygen species (ROS) through photogeneration. The incorporation of multiple benzothiadiazole units within the structure of cage **1** presents an excellent opportunity to harness white light for ROS generation in aqueous medium. Thus, from this viewpoint, cage **1** could be an excellent candidate for photocatalysis.

Our initial exploration focused on the oxidation reaction using methyl phenyl sulfide as a model substrate, employing aqueous cage **1** as the oxidizing agent (Scheme 3). Under aerobic conditions, the use of photocatalyst **1** resulted in the complete conversion of methyl phenyl sulfide to methyl phenyl sulfoxide within a remarkably short time frame of 4 h,

Scheme 3. Schematic Presentation of the Oxidation of Thioanisole

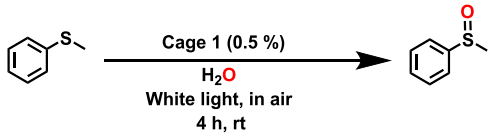

demonstrating outstanding selectivity in the process (Table 1, entry 2). Additionally, when subjected to comparable reaction

Table 1. Visible Light Oxidation of Sulfide to Sulfoxide

entry	catalyst	atmosphere	light	solvent	time (h)	yield (%)
1	1	O_2	+	H_2O	4	>99
2	1	air	+	H_2O	4	>99
3	1	air	−	H_2O	4	0
4	**1** + BQ	air	+	H_2O	4	>99
5	**1** + DABCO	air	+	H_2O	4	20
6	L	air	+	H_2O	4	10
7	L	air	+	CH_3CN	4	20
8	L_1	air	+	H_2O	4	0
9	[(tmeda) $Pd(NO_3)_2$]	air	+	H_2O	4	0

conditions, the ligand **L** alone was unable to catalyze the reaction (Table 1, entry 6−7). In the absence of light, no reaction was observed (Table 1, entry 3). In a control experiment utilizing DABCO as a quencher for singlet oxygen, only a 20% conversion was observed (Table 1, entry 5). The introduction of benzoquinone (BQ) did not result in a decline in the reaction's yield (Table 1, entry 4). Additionally, these findings suggest that the involvement of $^1O_2$ is more pivotal in the current reaction process compared to $O_2^{\bullet-}$. Therefore, under optimized conditions, methyl phenyl sulfide underwent nearly complete conversion to methyl phenyl sulfoxide within a concise 4 h time frame. To assess the substrate scope, diverse alkyl/aryl-substituted sulfides were subjected to the oxidation reaction by using the optimized conditions under visible light. All the alkyl/aryl-substituted sulfides exhibited the selective conversion to the corresponding sulfoxide through oxidation in very exceptionally high yields (Figure 5) without any trace of expected sulfones as byproducts.

In each case, the NMR and ESI mass spectra of the reaction mixtures were recorded after 4 h (Figures S13−S31). The turnover number for each substrate is 200. The catalyst's recyclability was then tested over 10 cycles after the reaction was concluded, demonstrating only negligible degradation in its catalytic performance (Figure S33). After each cycle, the

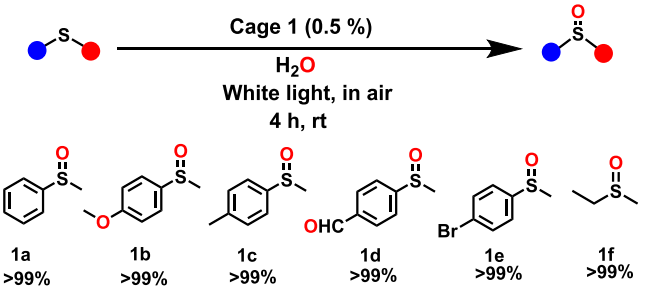

Figure 5. Visible light-driven oxidation of various sulfides.

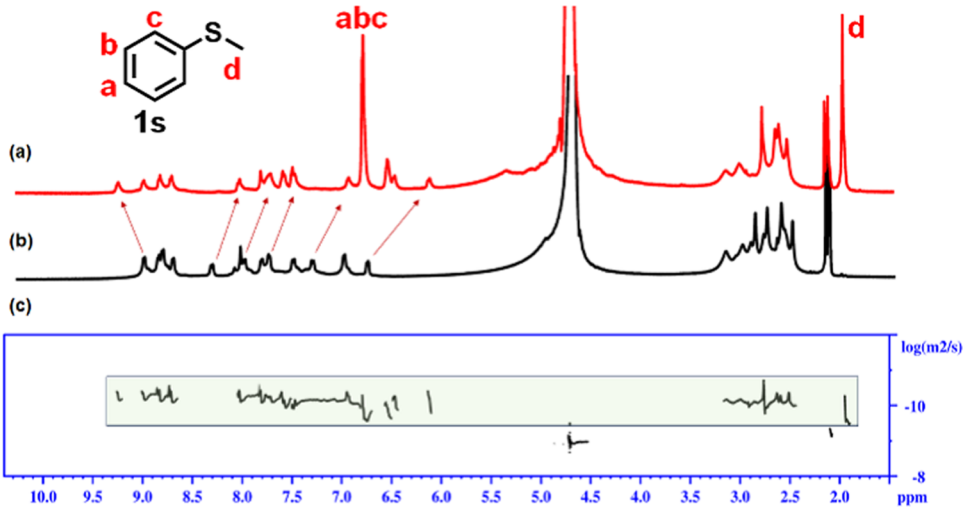

Figure 6. ^{1}H NMR stack plot of (a) **1** + **1s** in D_2O, (b) **1** in D_2O, and (c) diffusion-ordered ^{1}H NMR of **1** + **1s** in D_2O.

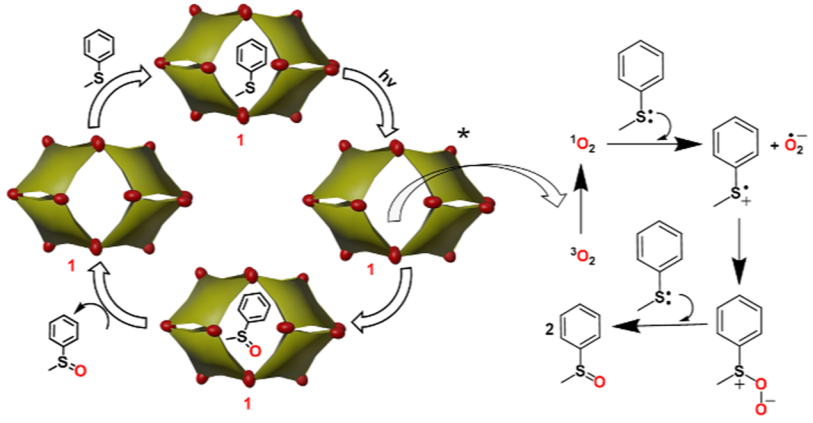

Figure 7. Plausible pathway for the $^{1}O_2$-promoted formation of sulfoxides in cage **1** in aqueous medium.

product was directly extracted from water by adding $CHCl_3$, as the cage is insoluble in $CHCl_3$. Following extraction, the substrate was reintroduced for the next cycle of catalysis, and the extraction process was repeated in subsequent cycles.

Additionally, we tested the possible binding of the substrate in the cage cavity, which could be a pivotal aspect of such high effectivity and selectivity of the catalysis. The encapsulation of methyl phenyl sulfide inside **1** leading to the formation of a host−guest adduct was confirmed by ^{1}H NMR where a shift of host peaks with the appearance of guest peaks was observed and a single diffusion band with a log *D* value of −10.148 was observed in the ^{1}H-DOSY analysis (Figure 6a−c). Furthermore, ^{1}H−^{1}H- NOESY (Figure S35) showed a clear interaction between the host and guest protons, which supports the encapsulation of the guest inside the cage's cavity. One may also expect binding of the guest at the external surface of the cage. To address this issue, four pyridine moieties of the ligand **L** were methylated followed by conversion to nitrate salt (**L1**) to prepare the water-soluble cationic form (**L1**) of the ligand **L**. If binding of a guest on the outer surface of the cage is possible, then, the same guest is expected to bind the cationic ligand **L1** in aqueous medium. Titration of methyl phenyl sulfide with **L1** in aqueous medium showed no change in the NMR pattern (Figure S38), which ruled out the external surface binding of the guest. The reaction of ethyl methyl sulfide in the presence of the cage (**1**) under similar reaction conditions resulted in the formation of sulfoxide selectively (Figure 5). If the guest binding was driven by $\pi-\pi$ interactions on the outer surface of the cage, dialkyl-substituted sulfide would not have shown such reactivity. Based on these findings, we can propose a mechanism where our cage acts as an enzyme-mimicking host and performs catalytic chemical transformation within the cage cavity (Figure 7). Thus, nanocage **1** provides an excellent platform for catalytic oxidation by allowing the substrate to get into the cage cavity and generating ROS.

CONCLUSIONS

In summary, we report here the successful construction of a water-soluble Pd_{16} nanocage through coordination self-assembly of a *cis*-Pd(II) 90° acceptor with a tetra-pyridyl donor (**L**) containing a benzothiadiazole core. An uncommon square orthobicupola structural topology, referred to as a 'Johnson polyhedral solid (J_{28}),' was established by structure analysis of **1** using single-crystal X-ray diffraction. To the best of our knowledge, complex **1** demonstrates the first instance of a water-soluble Pd(II) molecular architecture with a square orthobicupola geometry. The backbone of the nanocage incorporates several benzothiadiazole units, enabling it to be fluorescent, with the generation of ROS upon exposure to visible light in aqueous medium. Thus, cage **1** being a potential photocatalyst was used to address a challenging problem of

selective sulfide oxidation in water medium. The conventional approaches for this generally produce a mixture of sulfoxide and toxic sulfones. While sulfoxide is a crucial synthetic intermediate for biomolecules, the overoxidized sulfones are toxic, and their separation is difficult. Notably, nanocage **1** demonstrated excellent catalytic activity with selective aerial oxidation of aryl/alkyl sulfides to their corresponding sulfoxides under visible light in aqueous medium with very high yields, without the formation of toxic sulfones as byproducts. The products could be separated by simple filtration, and the aqueous solution of the catalyst could be reused up to 10 cycles without much loss of catalytic activity. Excellent photocatalytic activity in water for selective oxidation of sulfides to the corresponding sulfoxides combined with its unique structural topology makes the Pd_{16} nanocage (**1**) a promising example of functional self-assembled discrete architecture.

■ ASSOCIATED CONTENT

Supporting Information

The Supporting Information is available free of charge at https://pubs.acs.org/doi/10.1021/jacs.4c02956.

Experimental procedures, NMR spectra (^{1}H, COSY, NOESY, DOSY, ^{13}C), high-resolution ESI-MS, and photophysical analysis of the SCXRD data (PDF)
Crystallographic data (TXT)

Accession Codes

CCDC 2321537 contains the supporting crystallographic data for this paper. These data can be obtained free of charge via www.ccdc.cam.ac.uk/data_request/cif or by emailing data_request@ccdc.cam.ac.uk or by contacting The Cambridge Crystallographic Data Centre, 12 Union Road, Cambridge CB2 1EZ, U.K.; fax: +44 1223 336033.

■ AUTHOR INFORMATION

Corresponding Author

Partha Sarathi Mukherjee − *Department of Inorganic and Physical Chemistry, Indian Institute of Science, Bangalore 560012, India;* orcid.org/0000-0001-6891-6697; Email: psm@iisc.ac.in

Authors

Pranay Kumar Maitra − *Department of Inorganic and Physical Chemistry, Indian Institute of Science, Bangalore 560012, India*

Soumalya Bhattacharyya − *Department of Inorganic and Physical Chemistry, Indian Institute of Science, Bangalore 560012, India;* orcid.org/0000-0003-4467-6056

Neal Hickey − *Department of Chemical and Pharmaceutical Sciences, University of Trieste, Trieste 34127, Italy;* orcid.org/0000-0003-1271-5719

Complete contact information is available at: https://pubs.acs.org/10.1021/jacs.4c02956

Notes

The authors declare no competing financial interest.

■ ACKNOWLEDGMENTS

P.S.M. thanks the SERB-India for financial support as research grant and as J.C. Bose fellowship. P.K.M. is grateful to PMRF (India) for fellowship. The authors thank the DST-FIST for the NMR facility.

■ REFERENCES

(1) (a) Wong, C. H.; Whitesides, G. M. Enzyme-catalyzed transhydrogenation between nicotinamide cofactors and its application in organic synthesis. *J. Am. Chem. Soc.* **1982**, *104*, 3542−3544, DOI: 10.1021/ja00376a067. (b) Martí, S.; Roca, M.; Andrés, J.; Moliner, V.; Silla, E.; Tuñón, I.; Bertrán, J. Theoretical insights in enzyme catalysis. *Chem. Soc. Rev.* **2004**, *33*, 98−107, DOI: 10.1039/B301875J. (c) Bajaj, P.; Sreenilayam, G.; Tyagi, V.; Fasan, R. Gram-Scale Synthesis of Chiral Cyclopropane-Containing Drugs and Drug Precursors with Engineered Myoglobin Catalysts Featuring Complementary Stereoselectivity. *Angew. Chem., Int. Ed.* **2016**, *55*, 16110−16114, DOI: 10.1002/anie.201608680. (d) Winkler, M.; Geier, M.; Hanlon, S. P.; Nidetzky, B.; Glieder, A. Human Enzymes for Organic Synthesis. *Angew. Chem., Int. Ed.* **2018**, *57*, 13406−13423, DOI: 10.1002/anie.201800678.

(2) (a) Breslow, R.; Dong, S. D. Biomimetic Reactions Catalyzed by Cyclodextrins and Their Derivatives. *Chem. Rev.* **1998**, *98*, 1997−2012, DOI: 10.1021/cr970011j. (b) Meeuwissen, J.; Reek, J. N. H. Supramolecular catalysis beyond enzyme mimics. *Nat. Chem.* **2010**, *2*, 615−621, DOI: 10.1038/nchem.744. (c) Zhang, X.; Yang, C.; An, P.; Cui, C.; Ma, Y.; Liu, H.; Wang, H.; Yan, X.; Li, G.; Tang, Z. Creating enzyme-mimicking nanopockets in metal-organic frameworks for catalysis. *Sci. Adv.* **2022**, *8*, No. eadd5678, DOI: 10.1126/sciadv.add5678. (d) Sepehrpour, H.; Fu, W.; Sun, Y.; Stang, P. J. Biomedically Relevant Self-Assembled Metallacycles and Metallacages. *J. Am. Chem. Soc.* **2019**, *141*, 14005−14020, DOI: 10.1021/jacs.9b06222. (e) Feng, Q.; Li, R.; Gao, T.; Chu, D.; Zhang, M. Emissive metallacages for biomedical applications. *Sci. China Chem.* **2023**, *66*, 2447−2459, DOI: 10.1007/s11426-023-1672-4.

(3) (a) Ma, L.; Abney, C.; Lin, W. Enantioselective catalysis with homochiral metal−organic frameworks. *Chem. Soc. Rev.* **2009**, *38*, 1248−1256, DOI: 10.1039/b807083k. (b) Pluth, M. D.; Bergman, R. G.; Raymond, K. N. Proton-Mediated Chemistry and Catalysis in a Self-Assembled Supramolecular Host. *Acc. Chem. Res.* **2009**, *42*, 1650−1659, DOI: 10.1021/ar900118t. (c) Yoshizawa, M.; Klosterman, J. K.; Fujita, M. Functional Molecular Flasks: New Properties and Reactions within Discrete, Self-Assembled Hosts. *Angew. Chem., Int. Ed.* **2009**, *48*, 3418−3438, DOI: 10.1002/anie.200805340. (d) Cook, T. R.; Zheng, Y.-R.; Stang, P. J. Metal−Organic Frameworks and Self-Assembled Supramolecular Coordination Complexes: Comparing and Contrasting the Design, Synthesis, and Functionality of Metal−Organic Materials. *Chem. Rev.* **2013**, *113*, 734−777, DOI: 10.1021/cr3002824.

(4) (a) Breiner, B.; Clegg, J. K.; Nitschke, J. R. Reactivity modulation in container molecules. *Chem. Sci.* **2011**, *2*, 51−56, DOI: 10.1039/C0SC00329H. (b) Roy, B.; Devaraj, A.; Saha, R.; Jharimune, S.; Chi, K.-W.; Mukherjee, P. S. Catalytic Intramolecular Cycloaddition Reactions by Using a Discrete Molecular Architecture. *Chem. - Eur. J.* **2017**, *23*, 15704−15712, DOI: 10.1002/chem.201702507. (c) Kaphan, D. M.; Levin, M. D.; Bergman, R. G.; Raymond, K. N.; Toste, F. D. A supramolecular microenvironment strategy for transition metal catalysis. *Science* **2015**, *350*, 1235−1238, DOI: 10.1126/science.aad3087. (d) Martí-Centelles, V.; Lawrence, A. L.; Lusby, P. J. High Activity and Efficient Turnover by a Simple, Self-Assembled "Artificial Diels−Alderase. *J. Am. Chem. Soc.* **2018**, *140*, 2862−2868, DOI: 10.1021/jacs.7b12146. (e) Kaphan, D. M.; Toste, F. D.; Bergman, R. G.; Raymond, K. N. Enabling New Modes of Reactivity via Constrictive Binding in a Supramolecular-Assembly-Catalyzed Aza-Prins Cyclization. *J. Am. Chem. Soc.* **2015**, *137*, 9202−9205, DOI: 10.1021/jacs.5b01261.

(5) (a) Barry, N. P. E.; Zava, O.; Dyson, P. J.; Therrien, B. Excellent Correlation between Drug Release and Portal Size in Metalla-Cage Drug-Delivery Systems. *Chem. - Eur. J.* **2011**, *17*, 9669−9677, DOI: 10.1002/chem.201003530. (b) Schmitt, F.; Freudenreich, J.; Barry, N. P. E.; Juillerat-Jeanneret, L.; Süss-Fink, G.; Therrien, B. Organometallic Cages as Vehicles for Intracellular Release of Photosensitizers. *J. Am. Chem. Soc.* **2012**, *134*, 754−757, DOI: 10.1021/ja207784t. (c) Roy, I.; Bobbala, S.; Young, R. M.; Beldjoudi, Y.; Nguyen, M. T.; Cetin, M. M.; Cooper, J. A.; Allen, S.;

Anamimoghadam, O.; Scott, E. A.; Wasielewski, M. R.; Stoddart, J. F. A Supramolecular Approach for Modulated Photoprotection, Lysosomal Delivery, and Photodynamic Activity of a Photosensitizer. *J. Am. Chem. Soc.* **2019**, *141*, 12296−12304, DOI: 10.1021/jacs.9b03990. (d) Cosialls, R.; Simó, C.; Borrós, S.; Gómez-Vallejo, V.; Schmidt, C.; Llop, J.; Cuenca, A. B.; Casini, A. PET Imaging of Self-Assembled 18F-Labelled Pd2L4Metallacages for Anticancer Drug Delivery. *Chem. - Eur. J.* **2023**, *29*, No. e202202604, DOI: 10.1002/chem.202202604.

(6) (a) Chen, S.; Li, K.; Zhao, F.; Zhang, L.; Pan, M.; Fan, Y.-Z.; Guo, J.; Shi, J.; Su, C.-Y. A metal-organic cage incorporating multiple light harvesting and catalytic centres for photochemical hydrogen production. *Nat. Commun.* **2016**, *7*, No. 13169. (b) Acharyya, K.; Bhattacharyya, S.; Sepehrpour, H.; Chakraborty, S.; Lu, S.; Shi, B.; Li, X.; Mukherjee, P. S.; Stang, P. J. Self-Assembled Fluorescent Pt(II) Metallacycles as Artificial Light-Harvesting Systems. *J. Am. Chem. Soc.* **2019**, *141*, 14565−14569, DOI: 10.1021/jacs.9b08403. (c) Zhang, Z.; Zhao, Z.; Hou, Y.; Wang, H.; Li, X.; He, G.; Zhang, M. Aqueous Platinum(II)-Cage-Based Light-Harvesting System for Photocatalytic Cross-Coupling Hydrogen Evolution Reaction. *Angew. Chem., Int. Ed.* **2019**, *58*, 8862−8868, DOI: 10.1002/anie.201904407. (d) Jia, P.-P.; Xu, L.; Hu, Y.-X.; Li, W.-J.; Wang, X.-Q.; Ling, Q.-H.; Shi, X.; Yin, G.-Q.; Li, X.; Sun, H.; Jiang, Y.; Yang, H.-B. Orthogonal Self-Assembly of a Two-Step Fluorescence-Resonance Energy Transfer System with Improved Photosensitization Efficiency and Photooxidation Activity. *J. Am. Chem. Soc.* **2021**, *143*, 399−408, DOI: 10.1021/jacs.0c11370. (e) Li, Y.; Rajasree, S. S.; Lee, G. Y.; Yu, J.; Tang, J.-H.; Ni, R.; Li, G.; Houk, K. N.; Deria, P.; Stang, P. J. Anthracene−Triphenylamine-Based Platinum(II) Metallacages as Synthetic Light-Harvesting Assembly. *J. Am. Chem. Soc.* **2021**, *143*, 2908−2919, DOI: 10.1021/jacs.0c12853. (f) Acharyya, K.; Bhattacharyya, S.; Lu, S.; Sun, Y.; Mukherjee, P. S.; Stang, P. J. Emissive Platinum(II) Macrocycles as Tunable Cascade Energy Transfer Scaffolds. *Angew. Chem., Int. Ed.* **2022**, *61*, No. e202200715, DOI: 10.1002/anie.202200715. (g) Jia, P.-P.; Hu, Y.-X.; Peng, Z.-Y.; Song, B.; Zeng, Z.-Y.; Ling, Q.-H.; Zhao, X.; Xu, L.; Yang, H.-B. Construction of an Artificial Light-Harvesting System with Efficient Photocatalytic Activity in an Aqueous Solution Based on a FRET-Featuring Metallacage. *Inorg. Chem.* **2023**, *62*, 1950−1957, DOI: 10.1021/acs.inorgchem.2c01869. (h) Purba, P. C.; Maitra, P. K.; Bhattacharyya, S.; Mukherjee, P. S. Rigidification-Induced Emissive Metal−Carbene Complexes for Artificial Light Harvesting. *Inorg. Chem.* **2023**, *62*, 11037−11043, DOI: 10.1021/acs.inorgchem.3c01075.

(7) (a) Chen, S.; Chen, L.-J.; Yang, H.-B.; Tian, H.; Zhu, W. Light-Triggered Reversible Supramolecular Transformations of Multi-Bisthienylethene Hexagons. *J. Am. Chem. Soc.* **2012**, *134*, 13596−13599, DOI: 10.1021/ja306748k. (b) Han, M.; Michel, R.; He, B.; Chen, Y.-S.; Stalke, D.; John, M.; Clever, G. H. Light-Triggered Guest Uptake and Release by a Photochromic Coordination Cage. *Angew. Chem., Int. Ed.* **2013**, *52*, 1319−1323, DOI: 10.1002/anie.201207373. (c) Han, M.; Luo, Y.; Damaschke, B.; Gómez, L.; Ribas, X.; Jose, A.; Peretzki, P.; Seibt, M.; Clever, G. H. Light-Controlled Interconversion between a Self-Assembled Triangle and a Rhombicuboctahedral Sphere. *Angew. Chem., Int. Ed.* **2016**, *55*, 445−449, DOI: 10.1002/anie.201508307. (d) Chen, L.-J.; Yang, H.-B. Construction of Stimuli-Responsive Functional Materials via Hierarchical Self-Assembly Involving Coordination Interactions. *Acc. Chem. Res.* **2018**, *51*, 2699−2710, DOI: 10.1021/acs.accounts.8b00317. (e) Bhattacharyya, S.; Maity, M.; Chowdhury, A.; Saha, M. L.; Panja, S. K.; Stang, P. J.; Mukherjee, P. S. Coordination-Assisted Reversible Photoswitching of Spiropyran-Based Platinum Macrocycles. *Inorg. Chem.* **2020**, *59*, 2083−2091, DOI: 10.1021/acs.inorgchem.9b03572. (f) Chen, S.; Chen, L.; Cai, Y.; Zhu, W.-H. Photoswitchable Fluorescent Self-Assembled Metallacycles with High Photostability. *Chem. - Eur. J.* **2021**, *27*, 5240−5245, DOI: 10.1002/chem.202005184. (g) Hu, F.-L.; Wang, H.-F.; Guo, D.; Zhang, H.; Lang, J.-P.; Beves, J. E. Controlled formation of chiral networks and their reversible chiroptical switching behaviour by UV/microwave irradiation. *Chem. Commun.* **2016**, *52*, 7990−7993, DOI: 10.1039/C6CC03256G.

(8) (a) Chakrabarty, R.; Mukherjee, P. S.; Stang, P. J. Supramolecular Coordination: Self-Assembly of Finite Two- and Three-Dimensional Ensembles. *Chem. Rev.* **2011**, *111*, 6810−6918, DOI: 10.1021/cr200077m. (b) Wang, M.; Wang, C.; Hao, X.-Q.; Li, X.; Vaughn, T. J.; Zhang, Y.-Y.; Yu, Y.; Li, Z.-Y.; Song, M.-P.; Yang, H.-B.; Li, X. From Trigonal Bipyramidal to Platonic Solids: Self-Assembly and Self-Sorting Study of Terpyridine-Based 3D Architectures. *J. Am. Chem. Soc.* **2014**, *136*, 10499−10507, DOI: 10.1021/ja505414x. (c) Jiang, B.; Zhang, J.; Ma, J.-Q.; Zheng, W.; Chen, L.-J.; Sun, B.; Li, C.; Hu, B.-W.; Tan, H.; Li, X.; Yang, H.-B. Vapochromic Behavior of a Chair-Shaped Supramolecular Metallacycle with Ultra-Stability. *J. Am. Chem. Soc.* **2016**, *138*, 738−741, DOI: 10.1021/jacs.5b11409. (d) Gao, W.-X.; Feng, H.-J.; Guo, B.-B.; Lu, Y.; Jin, G.-X. Coordination-Directed Construction of Molecular Links. *Chem. Rev.* **2020**, *120*, 6288−6325, DOI: 10.1021/acs.chemrev.0c00321. (e) He, Y.-Q.; Fudickar, W.; Tang, J.-H.; Wang, H.; Li, X.; Han, J.; Wang, Z.; Liu, M.; Zhong, Y.-W.; Linker, T.; Stang, P. J. Capture and Release of Singlet Oxygen in Coordination-Driven Self-Assembled Organoplatinum(II) Metallacycles. *J. Am. Chem. Soc.* **2020**, *142*, 2601−2608, DOI: 10.1021/jacs.9b12693. (f) Wang, L.; Song, B.; Khalife, S.; Li, Y.; Ming, L.-J.; Bai, S.; Xu, Y.; Yu, H.; Wang, M.; Wang, H.; Li, X. Introducing Seven Transition Metal Ions into Terpyridine-Based Supramolecules: Self-Assembly and Dynamic Ligand Exchange Study. *J. Am. Chem. Soc.* **2020**, *142*, 1811−1821, DOI: 10.1021/jacs.9b09497. (g) Wang, L.-J.; Li, X.; Bai, S.; Wang, Y.-Y.; Han, Y.-F. Self-Assembly, Structural Transformation, and Guest-Binding Properties of Supramolecular Assemblies with Triangular Metal−Metal Bonded Units. *J. Am. Chem. Soc.* **2020**, *142*, 2524−2531, DOI: 10.1021/jacs.9b12309. (h) Díaz, A. E. M.; Lewis, J. E. M. Structural Flexibility in Metal-Organic Cages. *Front. Chem.* **2021**, *9*, No. 706462. (i) Raee, E.; Yang, Y.; Liu, T. Supramolecular structures based on metal-organic cages. *Giant* **2021**, *5*, No. 100050. (j) Li, X.-Z.; Tian, C.-B.; Sun, Q.-F. Coordination-Directed Self-Assembly of Functional Polynuclear Lanthanide Supramolecular Architectures. *Chem. Rev.* **2022**, *122*, 6374−6458, DOI: 10.1021/acs.chemrev.1c00602. (k) Sánchez-González, E.; Tsang, M. Y.; Troyano, J.; Craig, G. A.; Furukawa, S. Assembling metal−organic cages as porous materials. *Chem. Soc. Rev.* **2022**, *51*, 4876−4889, DOI: 10.1039/D1CS00759A. (l) Tateishi, T.; Yoshimura, M.; Tokuda, S.; Matsuda, F.; Fujita, D.; Furukawa, S. Coordination/metal−organic cages inside out. *Coord. Chem. Rev.* **2022**, *467*, No. 214612, DOI: 10.1016/j.ccr.2022.214612. (m) Luis, E. T.; Iranmanesh, H.; Arachchige, K. S. A.; Donald, W. A.; Quach, G.; Moore, E. G.; Beves, J. E. Luminescent Tetrahedral Molecular Cages Containing Ruthenium(II) Chromophores. *Inorg. Chem.* **2018**, *57*, 8476−8486, DOI: 10.1021/acs.inorgchem.8b01157.

(9) (a) Fujita, M.; Tominaga, M.; Hori, A.; Therrien, B. Coordination Assemblies from a Pd(II)-Cornered Square Complex. *Acc. Chem. Res.* **2005**, *38*, 369−378, DOI: 10.1021/ar040153h. (b) Debata, N. B.; Tripathy, D.; Chand, D. K. Self-assembled coordination complexes from various palladium(II) components and bidentate or polydentate ligands. *Coord. Chem. Rev.* **2012**, *256*, 1831−1945, DOI: 10.1016/j.ccr.2012.04.001. (c) Bhattacharyya, S.; Ali, S. R.; Venkateswarulu, M.; Howlader, P.; Zangrando, E.; De, M.; Mukherjee, P. S. Self-Assembled Pd12 Coordination Cage as Photoregulated Oxidase-Like Nanozyme. *J. Am. Chem. Soc.* **2020**, *142*, 18981−18989, DOI: 10.1021/jacs.0c09567. (d) Bhandari, P.; Modak, R.; Bhattacharyya, S.; Zangrando, E.; Mukherjee, P. S. Self-Assembly of Octanuclear PtII/PdII Coordination Barrels and Uncommon Structural Isomerization of a Photochromic Guest in Molecular Space. *JACS Au* **2021**, *1*, 2242−2248, DOI: 10.1021/jacsau.1c00361. (e) Cai, L.-X.; Yan, D.-N.; Cheng, P.-M.; Xuan, J.-J.; Li, S.-C.; Zhou, L.-P.; Tian, C.-B.; Sun, Q.-F. Controlled Self-Assembly and Multistimuli-Responsive Interconversions of Three Conjoined Twin-Cages. *J. Am. Chem. Soc.* **2021**, *143*, 2016−2024, DOI: 10.1021/jacs.0c12064. (f) Banerjee, R.; Bhattacharyya, S.; Mukherjee, P. S. Synthesis of an Adaptable Molecular Barrel and

Guest Mediated Stabilization of Its Metastable Higher Homologue. *JACS Au* **2023**, *3*, 1998−2006, DOI: 10.1021/jacsau.3c00224.
(10) (a) Fujita, N.; Biradha, K.; Fujita, M.; Sakamoto, S.; Yamaguchi, K. A Porphyrin Prism: Structural Switching Triggered by Guest Inclusion. *Angew. Chem., Int. Ed.* **2001**, *40*, 1718−1721, DOI: 10.1002/1521-3773(20010504)40:9<1718::AID-ANIE17180>3.0.CO;2-7. (b) Yamanoi, Y.; Sakamoto, Y.; Kusukawa, T.; Fujita, M.; Sakamoto, S.; Yamaguchi, K. Dynamic assembly of coordination boxes from (en) Pd (II) unit and a rectangular panel-like ligand: NMR, CSI-MS, and X-ray studies. *J. Am. Chem. Soc.* **2001**, *123*, 980−981, DOI: 10.1021/ja003043o. (c) Bar, A. K.; Chakrabarty, R.; Mostafa, G.; Mukherjee, P. S. Self-Assembly of a Nanoscopic Pt12Fe12 Heterometallic Open Molecular Box Containing Six Porphyrin Walls. *Angew. Chem., Int. Ed.* **2008**, *47*, 8455−8459, DOI: 10.1002/anie.200803543. (d) Wang, M.; Zheng, Y.-R.; Ghosh, K.; Stang, P. J. Metallosupramolecular Tetragonal Prisms via Multicomponent Coordination-Driven Template-Free Self-Assembly. *J. Am. Chem. Soc.* **2010**, *132*, 6282−6283, DOI: 10.1021/ja100889h. (e) Croué, V.; Goeb, S.; Szalóki, G.; Allain, M.; Sallé, M. Reversible Guest Uptake/Release by Redox-Controlled Assembly/Disassembly of a Coordination Cage. *Angew. Chem., Int. Ed.* **2016**, *55*, 1746−1750, DOI: 10.1002/anie.201509265. (f) Howlader, P.; Das, P.; Zangrando, E.; Mukherjee, P. S. Urea-Functionalized Self-Assembled Molecular Prism for Heterogeneous Catalysis in Water. *J. Am. Chem. Soc.* **2016**, *138*, 1668−1676, DOI: 10.1021/jacs.5b12237. (g) Ahmed, S.; Howlader, P.; Bhattacharyya, S.; Mondal, S.; Zangrando, E.; Mukherjee, P. S. Fluorescence enhancement via structural rigidification inside a self-assembled Pd4 molecular vessel. *Chem. Commun.* **2022**, *58*, 11390−11393, DOI: 10.1039/D2CC04561C.
(11) (a) Bar, A. K.; Mohapatra, S.; Zangrando, E.; Mukherjee, P. S. A Series of Trifacial Pd6Molecular Barrels with Porphyrin Walls. *Chem. - Eur. J.* **2012**, *18*, 9571−9579, DOI: 10.1002/chem.201201077. (b) Banerjee, R.; Chakraborty, D.; Mukherjee, P. S. Molecular Barrels as Potential Hosts: From Synthesis to Applications. *J. Am. Chem. Soc.* **2023**, *145*, 7692−7711, DOI: 10.1021/jacs.3c01084. (c) Purba, P. C.; Maity, M.; Bhattacharyya, S.; Mukherjee, P. S. A Self-Assembled Palladium(II) Barrel for Binding of Fullerenes and Photosensitization Ability of the Fullerene-Encapsulated Barrel. *Angew. Chem., Int. Ed.* **2021**, *60*, 14109−14116, DOI: 10.1002/anie.202103822. (d) Das, P.; Kumar, A.; Howlader, P.; Mukherjee, P. S. A Self-Assembled Trigonal Prismatic Molecular Vessel for Catalytic Dehydration Reactions in Water. *Chem. - Eur. J.* **2017**, *23*, 12565−12574, DOI: 10.1002/chem.201702263. (e) Bhattacharyya, S.; Venkateswarulu, M.; Sahoo, J.; Zangrando, E.; De, M.; Mukherjee, P. S. Self-Assembled PtII8Metallosupramolecular Tubular Cage as Dual Warhead Antibacterial Agent in Water. *Inorg. Chem.* **2020**, *59*, 12690−12699, DOI: 10.1021/acs.inorgchem.0c01777.
(12) (a) Cecot, G.; Marmier, M.; Geremia, S.; De Zorzi, R.; Vologzhanina, A. V.; Pattison, P.; Solari, E.; Tirani, F. F.; Scopelliti, R.; Severin, K. The Intricate Structural Chemistry of MII2nLn-Type Assemblies. *J. Am. Chem. Soc.* **2017**, *139*, 8371−8381, DOI: 10.1021/jacs.7b04861. (b) Sainaba, A. B.; Venkateswarulu, M.; Bhandari, P.; Clegg, J. K.; Mukherjee, P. S. Self-Assembly of an [M8L24]16+ Intertwined Cube and a Giant [M12L16]24+ Orthobicupola. *Angew. Chem., Int. Ed.* **2024**, *63*, No. e202315572, DOI: 10.1002/anie.202315572.
(13) Bhat, I. A.; Devaraj, A.; Zangrando, E.; Mukherjee, P. S. A Discrete Self-Assembled Pd12 Triangular Orthobicupola Cage and its Use for Intramolecular Cycloaddition. *Chem. - Eur. J.* **2018**, *24*, 13938−13946, DOI: 10.1002/chem.201803039.
(14) (a) Block, E. The organosulfur chemistry of the genus Allium−implications for the organic chemistry of sulfur. *Angew. Chem., Int. Ed. Engl.* **1992**, *31*, 1135−1178, DOI: 10.1002/anie.199211351. (b) Carreño, M. C. Applications of sulfoxides to asymmetric synthesis of biologically active compounds. *Chem. Rev.* **1995**, *95*, 1717−1760, DOI: 10.1021/cr00038a002. (c) Ferber, B.; Kagan, H. B. Metallocene sulfoxides as precursors of metallocenes with planar chirality. *Adv. Synth. Catal.* **2007**, *349*, 493−507, DOI: 10.1002/adsc.200600639. (d) Wojaczyńska, E.; Wojaczynski, J. Enantioselective synthesis of sulfoxides: 2000− 2009. *Chem. Rev.* **2010**, *110*, 4303−4356, DOI: 10.1021/cr900147h.
(15) (a) Hartz, R. A.; Arvanitis, A. G.; Arnold, C.; Rescinito, J. P.; Hung, K. L.; Zhang, G.; Wong, H.; Langley, D. R.; Gilligan, P. J.; Trainor, G. L. Synthesis and evaluation of 2-anilino-3-phenylsulfonyl-6-methylpyridines as corticotropin-releasing factor1 receptor ligands. *Bioorg. Med. Chem. Lett.* **2006**, *16*, 934−937, DOI: 10.1016/j.bmcl.2005.10.097. (b) Ilardi, E. A.; Vitaku, E.; Njardarson, J. T. Data-mining for sulfur and fluorine: An evaluation of pharmaceuticals to reveal opportunities for drug design and discovery: Miniperspective. *J. Med. Chem.* **2014**, *57*, 2832−2842, DOI: 10.1021/jm401375q.
(16) (a) Xu, X.; Huang, X.; Chang, Y.; Yu, Y.; Zhao, J.; Isahak, N.; Teng, J.; Qiao, R.; Peng, H.; Zhao, C.-X.; et al. Antifouling surfaces enabled by surface grafting of highly hydrophilic sulfoxide polymer brushes. *Biomacromolecules* **2021**, *22*, 330−339, DOI: 10.1021/acs.biomac.0c01193. (b) Yu, Y.; Xu, W.; Huang, X.; Xu, X.; Qiao, R.; Li, Y.; Han, F.; Peng, H.; Davis, T. P.; Fu, C.; Whittaker, A. K. Proteins conjugated with sulfoxide-containing polymers show reduced macrophage cellular uptake and improved pharmacokinetics. *ACS Macro Lett.* **2020**, *9*, 799−805, DOI: 10.1021/acsmacrolett.0c00291.
(17) (a) Shi, F.; Tse, M. K.; Kaiser, H. M.; Beller, M. Self-Catalyzed Oxidation of Sulfides with Hydrogen Peroxide: A Green and Practical Process for the Synthesis of Sulfoxides. *Adv. Synth. Catal.* **2007**, *349*, 2425−2430, DOI: 10.1002/adsc.200700206. (b) Yang, C.; Jin, Q.; Zhang, H.; Liao, J.; Zhu, J.; Yu, B.; Deng, J. Tetra-(tetraalkylammonium) octamolybdate catalysts for selective oxidation of sulfides to sulfoxides with hydrogen peroxide. *Green Chem.* **2009**, *11*, 1401−1405, DOI: 10.1039/b912521n. (c) Chinnusamy, T.; Reiser, O. A recyclable TEMPO catalyst for the aerobic oxidation of sulfides to sulfoxides. *ChemSusChem* **2010**, *3*, 1040−1042, DOI: 10.1002/cssc.201000105. (d) Yu, B.; Liu, A.-H.; He, L.-N.; Li, B.; Diao, Z.-F.; Li, Y.-N. Catalyst-free approach for solvent-dependent selective oxidation of organic sulfides with oxone. *Green Chem.* **2012**, *14*, 957−962, DOI: 10.1039/c2gc00027j.